Applied Clay Science 135 (2017) 611–619

Contents lists available at ScienceDirect

Applied Clay Science

journal homepage: www.elsevier.com/locate/clay

Research paper

Effects of lime treatments on marls

Kerstin Elert [a,*], Fernando Nieto [a,c], José Miguel Azañón [b,c]

[a] Department of Mineralogy and Petrology, University of Granada, Fuentenueva S/N, 18002 Granada, Spain
[b] Department of Geodynamics, University of Granada, Fuentenueva S/N, 18002 Granada, Spain
[c] IACT, CSIC-University of Granada, Spain

ARTICLE INFO

Article history:
Received 15 June 2016
Received in revised form 28 September 2016
Accepted 17 October 2016
Available online 10 November 2016

Keywords:
Soil stabilization
Smectite
C-(A)-S-H
Geotechnical properties
Carbonation
Marls

ABSTRACT

Marly clay was treated with calcitic and Mg-rich lime in order to determine the influence of the clay's high carbonate content on the stabilization effectiveness. The evolution of mineralogical and physical properties over the course of the treatment were studied using XRD, TEM, SEM, elemental analysis, TG, granulometry, and nitrogen sorption and correlated with the marly clay's improved geotechnical behaviour. Only a small portion of smectites and other clay minerals dissolved upon lime treatment. Changes in clay mineralogy had, thus, only very limited influence in the improvement of the material's plasticity and swelling behaviour, which was rather modified by an increase in particle size. This increase was primarily caused by aggregation induced by calcium silicate aluminium hydrate (C-(A)-S-H) formation, whereas flocculation had an only minor effect. After the initial improvement, disaggregation of clay particles occurred which resulted in a particle size decrease, most likely, caused by carbonation of C-(A)-S-H phases. These findings question the effectiveness of lime stabilization for marl using currently applied standard treatment protocols.

1. Introduction

Lime stabilization is the most common method to improve geotechnical properties of subgrades (Al-Mukhtar et al., 2012; Obuzor et al., 2012). The lime treatment modifies soil particle packing, soil plasticity, workability, dispersivity, swelling and shrinkage properties, settlement behaviour and permeability (Basma and Tuncer, 1991; Nalbantoglu and Tuncer, 2001; Seco et al., 2011a; Ouhadi et al., 2014). Even though, lime stabilization has been successfully employed for clayey soils, recent studies question its long-term effectiveness in the case of marly soils. An evaluation of geotechnical properties of marl stabilized with 2 wt% lime showed that plasticity and swelling pressure, which initially decreased, started to increase after prolonged curing at high pH and ambient temperature (Ureña et al., 2015).

Marl and marly clays contain clay minerals and carbonates in varying proportions from 20% to 55%. Marls have been generally classified following the same criteria used for the classification of clays and silts, while the presence of carbonates has not been taken into account. However, the presence of carbonates in these soils seems to be critical for their geotechnical behaviour. Lamas et al. (2002) proposed a characterization of the geotechnical properties of marls used for civil engineering purposes as a function of their carbonate content. Results of an investigation carried out by these authors revealed a strong relationship between expansion, plasticity, and reactivity and the carbonate and clay content of natural marls from south-eastern Spain.

Stabilization failure of marl has often been related to the presence of palygorskite and sepiolite which formed expansive minerals such as ettringite and thaumasite upon reaction in the presence of sulfates (Ouhadi and Yong, 2003). In recent years, however, studies on short and long-term mechanical properties of lime-stabilized marl showed relevant differences compared with those of lime-treated clayey soils. Sol-Sánchez et al. (2016) observed sensible differences in pH evolution and particle size distribution in lime stabilized marly and clayey soils from southern Spain. It is also widely accepted that stabilization is less effective and that higher lime concentration must conseqently be used to produce adequate mechanical properties in marl (e.g. Ghobadi et al., 2014; Ureña et al., 2015). As a response to doubts raised regarding the long-term effectiveness of lime treatments, the suitability of alternative additives for the stabilization of marl has been studied in recent years (Guney et al., 2007; Seco et al., 2011b; Ureña et al., 2013, 2015).

Although, there is no conclusive answer to this anomalous behaviour, the high carbonate concentration of marl might be the responsible factor. Carbonates can act as a pH buffer, resulting in a premature reduction in pH and, thus, limiting long-term mineralogical changes in clay minerals subjected to lime treatment. In this work, we investigate the use of calcitic and magnesium-rich lime to improve geotechnical properties of highly expansive marl which outcrop in southern Spain, producing landslides and severe damage to highway subgrades (Azañón et al., 2010). This laboratory study analyses the mechanisms of lime stabilization in marl in order to establish their short and long-term

* Corresponding author.
E-mail address: kelert@ugr.es (K. Elert).

http://dx.doi.org/10.1016/j.clay.2016.10.047
0169-1317/

physico-chemical behaviour. Possible factors triggering the deterioration of geotechnical properties of lime-treated marl over time are discussed.

2. Materials and methods

2.1. Materials

2.1.1. Marl sample

A sample of natural marly clay which is part of a Flysch-type formation outcropping in the south of Spain has been selected for this study. This formation represents a turbiditic sequence of Cretaceous–Lower Miocene age that outcrops continuously in the western and central parts of the Betic Cordillera (Bourgois et al., 1974). From a geotechnical point of view, this formation is well known because it is the origin of multiple slope instabilities and road damages. The material used in this study has been extracted by drilling (32 m depth) and it belongs to clay-rich levels located at the base of the Diezma (Granada, Spain) landslide (Azañón et al., 2010). These clay-rich levels have been extensively studied from geotechnical and mineralogical perspectives (Nieto et al., 2008; Azañón et al., 2010).

2.1.2. Additives

In this study we used a commercial hydrated lime (CL-90-Q according to the Spanish Standard UNE-EN 459-1 (AENOR, 2011)) as well as a hydrated magnesium-rich lime obtained from calcined and hydrated residual sludge from the extraction of magnesium-rich limestone and marble which are abundant in the location of the test site. The use of this waste material, mainly composed of Ca and Mg hydroxide, could reduce economic cost of soil stabilization and improve the waste management process.

2.1.3. Sample treatment

Marl samples were mixed with calcitic or magnesium-rich limes in proportions of 5, 10 and 15 wt%. Hundred fifty grams of dry sample and the corresponding amount of dry additive were thoroughly mixed for 10 min. Water was added until reaching the plastic limit and the mixture was blended in an industrial mixer for 10 min. Samples were kept under laboratory conditions (i.e., air exposure and room T in order to simulate field application). Water was added when necessary to keep samples completely covered during the experimental run. Samples for analysis were taken and the pH of the solution was measured at 7, 14, 21, 49, 77, 105 and 201 days. In order to keep the conditions as much as possible similar to those of the test side, the samples were only stirred prior to the collection of aliquots.

2.2. Analytical techniques

2.2.1. X-ray fluorescence

Elemental analysis of decarbonated marl and additives was performed using a wavelength dispersive X-ray fluorescence spectrometer (BRUKER S4 Pioneer).

2.2.2. pH measurements

The pH of marl-lime mixtures was measured over the course of the experiment using a pH-meter Stick Piccolo HI 1280 (Hanna Instruments).

2.2.3. Geotechnical characterization

Geotechnical properties of untreated marl and marl-lime mixtures cured for 201 days were determined. The Atterberg consistency limits (i.e., liquid (LL) and plastic limit (PL)) were established in accordance with Spanish standards UNE 103103 (AENOR, 1994) and UNE 103104 (AENOR, 1993). The plasticity index (PI) is obtained according to the following formula: $PI = LL - PL$.

The Spanish Standard UNE 103602 (AENOR, 1996) was followed to determine the swelling pressure and the ASTM standard D2435 (ASTM, 2004) was used to measure free swell of the original untreated marl and all the mixtures prepared in this study. All samples were tested at optimum moisture content (OMC = 39.1%) determined by the Standard Proctor compaction test (ASTM, 2012).

2.2.4. Particle size analysis

Particle size analysis of powder samples dispersed in alcohol was performed using a Mastersizer 2000LF (Malvern Instruments). This instrument measures particles in the range 0.02–1500 μm using laser diffraction.

2.2.5. Surface area measurements (BET)

Nitrogen sorption isotherms of powdered samples before and after lime stabilization were obtained at 77 K on a TriStar 3000 equipment (Micromeritics). About 0.2 g of sample was degassed at 80 °C for 24 h prior to analysis using a sample degas system (VacPrep 061, Micrometrics). Note that the pre-treatment was conducted at 80 °C to avoid structural changes in clay minerals/smectites. The surface area of untreated and treated marly clay samples was determined using the BET method (Brunauer et al., 1938).

2.2.6. X-ray diffraction

The untreated and treated samples were studied by means of X-ray diffraction (XRD), using a PANalytical X'Pert Pro diffractometer (CuKα radiation, 45 kV, 40 mA) equipped with an X'Celerator solid-state linear detector, using a step increment of 0.008° 2θ and a counting time of 10 s/step. In the case of superposed peaks, the identification of phases and the measurement of intensities of each individual peak were carried out with the help of decomposition routines included in the MacDiff software (Petschick, 2010). Intensities were measured using peak areas. Four types of specimens were prepared and studied: disoriented powders, oriented aggregates (OA) smeared onto glass slides of whole samples, OA of Mg-exchanged samples, and OA of <2 μm fraction separated by centrifugation using a Kubota KS8000. Centrifugation time was 100 s. at 1000 rpm.

2.2.7. Determination of the smectite proportion by thermogravimetry

The smectite content (Sme%) of the original and treated samples was determined by thermogravimetric analysis (TG) according to the methodology developed by Nieto et al. (2008). The method consists in measuring the weight loss between 100 and 450 °C (WL) of samples solvated with ethylene glycol (EG) and previously saturated with Mg. The proportion of expandable material was calculated according to the following equation: $Sme\% = 3.96\ WL - 4.05$, which was established using artificial mixtures prepared with variable proportions of smectite. Note that the equation is in agreement with the theoretical proportion of EG in a solvated smectite (Nieto et al., 2008). The dry and disaggregated samples were spread in Petri capsules and exposed to EG vapours at 60 °C for 3 days. TG analyses were performed on ~40 mg of sample in air (50 ml/min flow rate), at a constant heating rate of 5 °C/min using a Shimadzu TGA-50H. TG analysis was also performed on some representative samples without the EG treatment in order to check for possible interference of weight losses upon thermal degradation of newly formed mineral phases (i.e., calcium silicate hydrate (C-S-H) or calcium silicate aluminium hydrate (C-A-S-H)). TG curves of the different unsolvated samples fully overlapped in the region from 100 to 450 °C and no additional peaks were detected in DTG traces. Based on these results any interference can be ruled out.

2.2.8. Elemental analysis

Elemental analysis (EA) of carbon was performed to verify carbonate content of untreated and treated marl using a Fisons Carlo Erba EA 1108 CHNS O equipped with TCD detection system. The samples were heated

to 1020 °C during 800 s and calculations were carried out employing Eager 200 software.

2.2.9. SEM

Powdered untreated and treated samples were coated with 50 Å of carbon and examined with a Zeiss SUPRA40VP scanning electron microscope (SEM), using secondary electrons. Qualitative analyses were obtained with an Oxford energy dispersive X-ray spectroscopy (EDS) microanalyzer.

2.2.10. TEM

Transmission electron microscopy (TEM) and high-resolution transmission electron microscopy (HRTEM) studies of untreated and treated samples were performed. Powdered samples were deposited on holey C-coated Au grids. Two microscopes were used: a Philips CM20, operating at 200 kV and a Titan with XFEG emission gun, spherical aberration corrector and HAADF detector, working at 300 kV, with a resolution of 0.8 Å in the TEM mode and 2 Å in the scanning transmission electron microscopy (STEM) mode. Quantitative chemical analyses (TEM-AEM) were obtained in STEM mode, with an EDAX solid-state energy dispersive X-ray (EDX) detector in the CM20 and a SuperX detector in the Titan. In the case of the CM20, a scan window of ~20 × 100 nm was used for the analysis of individual clay particles. In the case of the Titan, compositional maps were obtained of the entire analyzed area. For this task, individual spectra corresponding to each pixel of homogeneous areas were summed up to produce the average spectrum of the entire analyzed area. Albite, biotite, muscovite, spessartine, olivine and titanite standards were used to obtain K-factors for the transformation of intensity ratios to concentration ratios according to Cliff and Lorimer (1975). The structural formulae of smectite were calculated on the basis of 22 negative charges, i.e. $O_{10}(OH)_2$. All the Fe was considered as trivalent.

3. Results

3.1. X-ray fluorescence

The chemical composition of the carbonate-free fraction of the marly clay sample and of both types of hydrated lime is shown in Table 1. The marly clay and lime composition are consistent with the mineralogical composition determined using XRD (see below). The carbonate content was determined using elemental analysis (see below).

3.2. Evolution of pH during the treatments

Almost all samples reached pH values ~12.5 immediately after the addition of lime (Fig. 1). As expected, the pH decreased progressively over the course of the treatment, reaching values ranging from 10 to 11 after 201 days. The sample treated with 5 wt% calcitic lime showed comparatively lower pH values starting at 11.7 and quickly decreasing to <10. The final pH of this treatment was 8. The decrease in pH was generally more gradual for the two treatments at 15 wt% lime concentration, showing a slower, less abrupt reduction during the first 50 days than the treatments using lower lime concentrations.

Table 1
Chemical analyses of decarbonated marly clay and additives (wt%).

	Decarbonated marly clay	Calcitic lime	Mg-rich lime
SiO_2	64.23	0.39	0.84
Al_2O_3	13.15	0.21	0.36
Fe_2O_3	6.05	0.09	0.54
MnO	0.03	0.00	0.05
MgO	2.12	0.51	25.26
CaO	0.81	66.50	54.21
Na_2O	0.19	0.00	0.00
K_2O	2.92	0.06	0.05
TiO_2	0.66	0.01	0.02
P_2O_5	0.06	0.04	0.00
Loss on ignition	9.63	31.03	18.60

3.3. Geotechnical properties

The geotechnical properties of untreated marly clay and treated samples are shown in Table 2. The marly clay is highly plastic and extremely expansive. The liquid and plastic limits were 67 and 24.3, respectively. The dry unit weight was 1.39 kN/cm^3. After 201 days of curing, treated marly clay showed a noteworthy reduction in plasticity. The liquid limit suffered a reduction in almost all samples and the plastic limit showed an increase. These changes produced a substantial reduction of the plasticity index, which was proportional to the lime concentration of the treatments. The dry unit weight for treated marly clay is lower than that of the untreated marly clay. Therefore, both, free swell and swelling pressure, are drastically reduced after curing for 201 days.

3.4. Particle size analysis

Particle size analysis revealed an immediate shift in the particle size maximum from 10 μm in the untreated marl to 15–18 μm, depending on type and concentration of lime (Table 3). After 1 week of treatment, a further important increase of the particle size maximum was detected which was proportional to the lime concentration, the Mg-rich lime always being more effective in increasing the particle size. After 105 days the maximum particle size was achieved and further treatment resulted in a particle size decrease in almost all treated samples.

3.5. Surface area measurement (BET)

The calculated BET surface area of the original marl sample was 39.19 m^2/g. Calcitic and magnesium-rich lime had a surface area of 2.82 and 9.91 m^2/g, respectively. Nitrogen sorption measurements indicate an immediate decrease in BET surface area of ~45–70% upon lime treatment (Table 4). A correlation between surface area reduction and amount of lime added can be observed. Higher concentrations of lime resulted in a more significant surface area decrease. However, the observed decrease cannot only be associated with the reduction caused by mixing the marl with an agent of lower surface area. Considering the mixing ratios, final surface areas would be between 33.5 and 37.5 m^2/g, depending on lime type and concentration. After the first week of treatment an important surface area increase of between 70 and 170% could be detected in all samples, depending on the amount of lime added to the marl. During the first 3 months of treatment, the surface area of all samples suffered minor fluctuations, which, in part, might have been caused by a certain inhomogeneity of the samples. However, all samples experienced a minor surface area increase between 3 and 6 months of treatment. The final surface area was highest in samples treated with 5 wt% calcitic and Mg-rich lime.

3.6. X-ray diffraction

XRD analyses showed that the untreated marl mainly contained clay minerals, quartz, calcite and trace amounts of feldspar and dolomite. Smectite was the dominant clay mineral together with minor amounts of mica and kaolinite. Smectite identification was corroborated through EG treatment.

Qualitatively, only minor changes were observed in the XRD patterns of the bulk sample and the clay fraction of samples treated with calcitic or Mg-rich lime at various concentrations. Samples treated with high concentrations of Mg-rich lime contained small amounts of brucite. Portlandite was not detected, suggesting a complete carbonation or transformation of calcium hydroxide upon reaction with clay minerals. XRD analysis did not allow the detection of C-(A)-S-H phases in the bulk sample or in the clay fraction due to their scarcity and

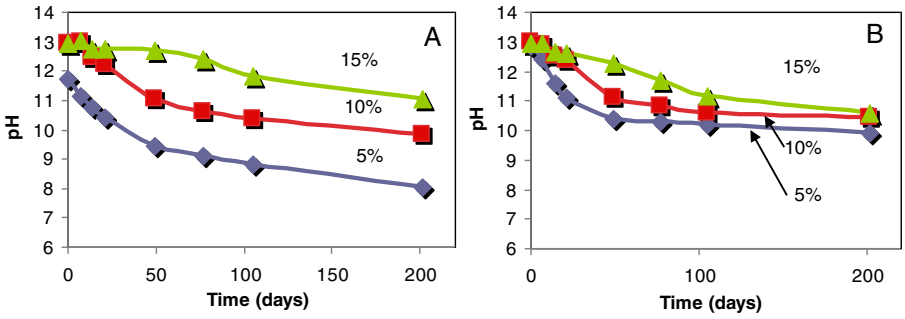

Fig. 1. Evolution of pH of marl treated with different concentrations of A) calcitic lime and B) Mg-rich lime.

amorphous character. XRD patterns of EG solvated samples revealed that the intracrystalline swelling of smectites was not significantly modified upon lime treatment.

To determine whether clay minerals suffered preferential dissolution upon lime treatment, the intensities of the peak (100) of quartz at 4.26 Å and that at 4.48 Å, which is the general (*hkl*) reflection present in most of the phyllosilicates and usually employed in quantitative analysis (Moore and Reynolds, 1989), were measured and compared among the different treatments (Fig. 2). The intensity ratio of untreated samples suffered a slight decrease during the first week of treatment from 1.36 to ~1.2, which corresponds to a reduction in clay minerals of ~13%. Further treatment did not result in any additional systematic decrease or any meaningful differences among the various lime treatments. The individual non-systematic differences can be explained by the only approximate character of semi-quantitative XRD analysis when minerals of different morphologies are studied (Moore and Reynolds, 1989).

Some minor differences in the position (basal d_{001} spacing) of smectite were visible in the total and the <2 μm fraction of oriented aggregates. However, such differences disappeared when the specimens were homoionized with Mg. Hence they were the result of differences in the interlayer exchangeable cations and/or hydration state of the smectites (Moore and Reynolds, 1989).

Interestingly, the overall quantity of the <2 μm fraction that was possible to extract from the treated samples using centrifugation, was dramatically reduced. This produced anomalous XRD patterns, showing clearly lower-intensity peaks for all of the phyllosilicates after only 7 days of lime treatment (Fig. 3). A similar behaviour has been observed by Ouhadi et al. (2014). Apparently, the extracted fraction had low clay mineral content and was in great part formed by amorphous material and minor amounts of minerals commonly associated with bigger-size fractions.

3.7. Determination of the smectite content by thermogravimetry

According to TG analysis of EG solvated samples, the untreated marl had an average smectite content of 30.5 ± 2.0 wt%. Untreated samples, generally, had slightly lower smectite content, the average being 28.4 ± 2.1 wt%. However, samples did not experience a systematic decrease in smectite content over the course of the treatment (Fig. 4) and no important differences were observed among the various treatments (i.e., different type or concentration of lime). Considering the smectite content of the untreated sample, we conclude that lime treatments did only produce dissolution of a small amount of smectite, close to the detection limit of this method (Nieto et al., 2008). TG analysis also confirmed XRD results, suggesting the scarcity of C-(A)-S-H phases which did not cause any significant weight loss upon thermal degradation.

Table 2
Geotechnical properties of untreated marly clay and marly clay treated with calcitic and Mg-rich lime of varying concentrations for 201 days.

		Calcitic lime			Mg-rich lime		
	Untreated	5 wt%	10 wt%	15 wt%	5 wt%	10 wt%	15 wt%
Dry unit weight (kN/cm^3)	1.39	–	–	1.02	–	1.17	–
Free swell (%)	8.6	–	–	1.9	–	0.6	–
Swelling pressure (kPa)	500	–	–	210	–	40	–
Liquid limit	67.0	69.5	51.0	70.8	60.7	53.8	51.2
Plastic limit	24.3	23.8	41.2	56.9	29.1	36.0	46.8
Plasticity index	42.7	45.7	9.8	13.9	31.5	17.8	4.5

3.8. Elemental analysis

EA results revealed that the untreated marly clay had a carbonate content of 24.4 wt%. The addition of 15 wt% of calcitic or magnesium-rich lime resulted in a rapid increase in carbonate content to 27.9 and 29.5 wt%, respectively (Table 5). Over the course of the treatment no clear evidence of an additional increase in carbonates was observed. Fluctuations in carbonate content were detected which are due to experimental errors and/or a certain inhomogeneity of the samples.

3.9. SEM

Secondary electron images of the untreated sample showed disaggregated particles of the previously described constituent minerals. The clay-rich areas were formed by individual, separated particles of smectite, showing a characteristic platy morphology (Fig. 5A). The particles were homogeneous in form and size (i.e., slightly less than 1 μm long and around 10 nm thick) and their mineralogical nature was confirmed by EDX microanalysis.

Samples treated with calcitic lime revealed a completely different texture if compared with untreated samples (Fig. 5B), showing the ubiquitous presence of a continuous layer of material with a non-defined morphology, which cemented the smectite particles. Smectite particles had the same size and chemical composition as those of the untreated sample. According to EDX microanalysis, the cementing material contained Si and Ca in similar proportion, together with O and Al as the main elements. Therefore, it was preliminarily interpreted as

Table 3
Particle size maximum (μm) of marl treated with calcitic and Mg-rich lime of varying concentrations.

	Calcitic lime			Mg-rich lime		
Time (days)	5 wt%	10 wt%	15 wt%	5 wt%	10 wt%	15 wt%
0	15	15	18	13	14	17
7	20	28	33	29	34	38
49	20	36	35	41	39	47
105	20	38	40	39	50	80
201	17	39	38	30	45	60

Table 4
Surface area (m^2/g) of marl treated with calcitic and Mg-rich lime of varying concentrations.

	Calcitic lime			Mg-rich lime		
Time (days)	5 wt%	10 wt%	15 wt%	5 wt%	10 wt%	15 wt%
0	16.2	12.6	11.2	21.2	18.5	14.0
7	38.7	32.8	29.9	35.4	32.8	34.4
14	35.3	35.3	25.4	36.9	34.3	30.1
49	40.7	27.8	20.9	34.3	29.9	27.0
105	43.2	29.8	35.7	38.8	31.4	29.6
201	44.4	32.1	38.4	51.1	35.7	36.9

C-(A)-S-H. This interpretation was confirmed during TEM examination (see below). In samples treated with 15 wt% Mg-rich lime, newly formed $CaCO_3$ crystals were identified.

3.10. TEM

TEM images of the untreated sample showed all the characteristics and textural features (i.e., aggregates and flakes of irregular and undulated outlines) commonly described in the geological literature for marls (Nieto et al., 1996). Smectite particles were observed either dispersed or forming monomineralic clusters of numerous individual irregular particles. Their composition, determined by AEM, allowed their classification as a solid solution between the extreme terms montmorillonite and beidellite, with a minor nontronitic component (Table 6). No other minerals or phases different of those determined by XRD were observed.

TEM analysis provided unambiguous evidence for the formation of C-(A)-S-H phases in samples treated with 15 wt% calcitic lime for 7 days (Fig. 6). Neither well-defined spots nor Debye rings were present in electron diffraction patterns of areas formed by C-(A)-S-H which produced the characteristic diffuse haloes of amorphous material (Fig. 6, inset). In samples treated with only 5 wt% calcitic lime, in contrast, C-(A)-S-H phases were not detected at any stage of the treatment. Note that TEM results of samples treated with 10 wt% lime are not reported here because they do not provide any additional information.

Samples treated with 15 wt% calcitic or Mg-rich lime for 201 days suffered important textural changes. Neither individual smectite particles nor monomineralic clusters were observed and all smectite particles formed aggregates with C-(A)-S-H (Fig. 7A and B). Clay particles were surrounded by the newly formed C-(A)-S-H phase which acted as a cementing material (Fig. 8). In practice, obtaining pure-smectite compositions by routine AEM, in a similar way to that described for untreated samples, revealed impossible due to their fine-scale mixing with C-(A)-S-H. Only after processing a set of spectra obtained from homogeneous areas selected on compositional maps obtained after long

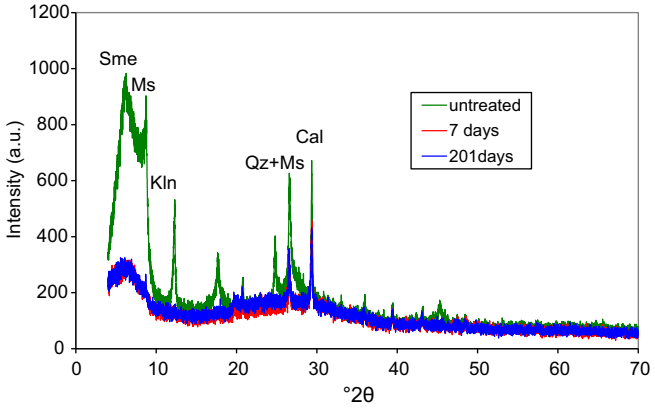

Fig. 3. XRD patterns of the <2 μm fraction of the untreated sample and the sample treated with 15 wt% calcitic lime during 7 and 201 days. Mineral abbreviations according to Whitney and Evans (2010); Ms = unspecified micas.

counting times (Fig. 7B), it was possible to determine the composition of smectites. They did not show any systematic difference compared to compositions obtained for the untreated sample (Table 6). Smectitic areas were also recognized by their characteristic diffraction and lattice fringe images of packets of 11 Å layers (Fig. 7C). High-resolution images of the C-(A)-S-H areas (obtained using the same routine as for smectite in Fig. 7C) showed a complete lack of periodicity, even at short range (Fig. 7E) and were interpreted as fully amorphous (Fig. 7D). The disordered, non-crystalline character generated sharp compositional differences from area to area, well recognizable in the compositional maps of Ca (Fig. 7B), Al and Si. The Ca/Si ratio ranged from 0.3 to 1.3 (Table 7). During TEM analysis, the degree of structural order of C-(A)-S-H changed over time in some of the areas as a result of electron irradiation. Small areas of disoriented crystals were observed, whose diffraction characteristics were coherent with those of a tobermorite-type phase, a crystalline variety of C-S-H (Biagioni et al., 2016).

4. Discussion

4.1. Mineralogical changes upon lime treatment

The experimental results revealed significant mineralogical changes in lime-treated marly clay, which resulted in improved engineering properties. These changes included limited clay mineral dissolution and the formation of C-(A)-S-H phases. Additionally, carbonation of $Ca(OH)_2$ led to the formation of calcite. Mineral dissolution in alkaline environments primarily affects clay minerals such as smectites and

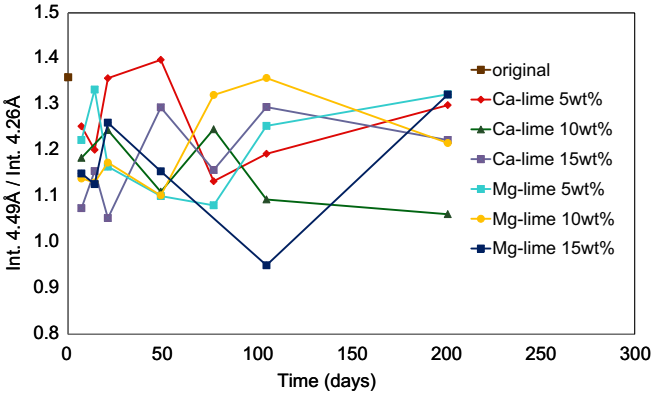

Fig. 2. Evolution of the intensity ratios between the 4.4 Å general reflection of phyllosilicates and of quartz at 4.26 Å for samples treated with 5, 10 and 15 wt% of calcitic or Mg-rich lime.

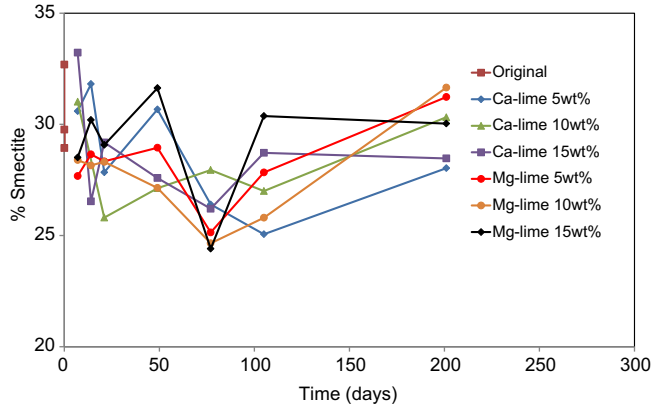

Fig. 4. Evolution of the smectite content determined by thermogravimetry of EG solvated samples according to the method by Nieto et al. (2008).

Table 5
Carbonate content of marly clay treated with 15 wt% of calcitic and Mg-rich lime.

Time (days)	Calcitic lime	Mg-rich lime
0	27.9	29.5
7	29.5	24.9
21	32.7	30.2
49	27.0	25.9
77	30.4	24.4
105	29.4	23.6
201	29.4	24.0

kaolinite (Carroll and Starkey 1971). XRD results showed a reduction in the clay mineral (i.e., smectite, kaolinite, and mica) content of ~13%, which occurred during the first week of lime treatment. Further treatment did not result in any additional systematic decrease in the clay mineral content. XRD patterns of the <2 μm fraction of samples treated for 7 and 201 days were identical and showed drastic modifications as compared to the XRD pattern of the untreated sample (Fig. 3). It was concluded that these modifications were not only due to clay mineral dissolution but also the result of short-term flocculation and aggregation effects, leading to the formation of >2 μm clay/C-(A)-S-H aggregates which caused a reduction in clay content in the <2 μm fraction. Thermogravimetric analysis of EG solvated samples confirmed XRD results, revealing a minor reduction in smectite content of ~9 wt% upon lime treatments (Fig. 4). These results indicate that the pH induced dissolution process affected an only small proportion of the marl's clay content, most likely the fine-grained material which is preferentially dissolved (Huertas et al. 1999). The observed improvement in the mechanical properties of lime-treated marl can, thus, not chiefly be attributed to the chemical destruction of smectite.

According to SEM analysis smectite particles did not suffer any important morphological changes. However, these particles were surrounded and cemented by a C-(A)-S-H phase identified by EDS microanalysis. The lack of morphological changes suggests that a pseudomorphic replacement had occurred which preserved the overall shape of the clay particle, only transforming a thin superficial layer into C-(A)-S-H. This finding is consistent with TEM observations which revealed that clay particles were completely surrounded by the cementing C-(A)-S-H phase (Fig. 8). Pseudomorphic replacements

Table 6
Structural formulae (AEM-TEM) of smectite from untreated marl and marl treated with 15 wt% calcitic lime based on $O_{10}(OH)_2$.

Si	^{IV}Al	^{VI}Al	Mg	Fe	Σ Oct.[a]	Na	K	Ca	Σ Int.[b]
Smectite from untreated marl									
3.97	0.03	1.38	0.28	0.33	1.99	0.00	0.21	0.07	0.35
3.91	0.09	1.06	0.42	0.49	1.97	0.07	0.37	0.09	0.62
3.80	0.20	1.20	0.38	0.45	2.03	0.00	0.31	0.09	0.49
3.80	0.20	1.47	0.28	0.33	2.08	0.00	0.16	0.05	0.26
3.73	0.27	1.63	0.33	0.17	2.13	0.00	0.12	0.05	0.23
3.67	0.33	1.20	0.32	0.49	2.01	0.00	0.49	0.07	0.63
3.66	0.34	1.23	0.33	0.47	2.03	0.00	0.39	0.09	0.57
3.49	0.51	1.39	0.37	0.33	2.09	0.00	0.41	0.11	0.62
3.42	0.58	1.44	0.23	0.41	2.08	0.00	0.55	0.02	0.59
3.42	0.58	1.34	0.19	0.63	2.16	0.00	0.23	0.04	0.30
Smectite from marl treated with 15 wt% calcitic lime for 201 days									
3.76	0.24	1.11	0.40	0.49	2.00	0.00	0.42	0.12	0.65
3.75	0.25	1.19	0.51	0.36	2.06	0.00	0.40	0.09	0.58
3.70	0.30	0.98	0.64	0.53	2.15	0.00	0.29	0.10	0.48
3.58	0.42	1.58	0.23	0.27	2.08	0.00	0.25	0.08	0.41
3.48	0.52	1.54	0.37	0.19	2.10	0.00	0.43	0.08	0.59

[a] Sum of octahedral cations.
[b] Sum of interlayer charge.

have been observed during the dissolution of most silicate minerals including feldspars, olivines, pyroxenes and phyllosilicates (Putnis, 2009; Zauyah et al., 2010).

TEM-AEM analyses disclosed that the chemical composition of smectites was not affected by the lime treatment after 201 days (Table 6). Furthermore, this technique allowed the unambiguous detection of C-(A)-S-H amorphous phases formed after only 7 days of treatment (Fig. 6) as well as their chemical characterization (Table 7). C-S-H phases have frequently been observed as a reaction product in smectite experimentally altered under alkaline conditions (Gaucher and Blanc, 2006; Al-Mukhtar et al., 2012). Their crystalline, semi-crystalline or amorphous nature has often been a matter of controversy. Such controversy might not only be the consequence of a lack of scientific evidence, but most probably reflects actual variability in the nature of these phases (Richardson, 2008, 2014). Electron diffraction allowed us to determine the amorphous nature of the C-(A)-S-H phase formed during

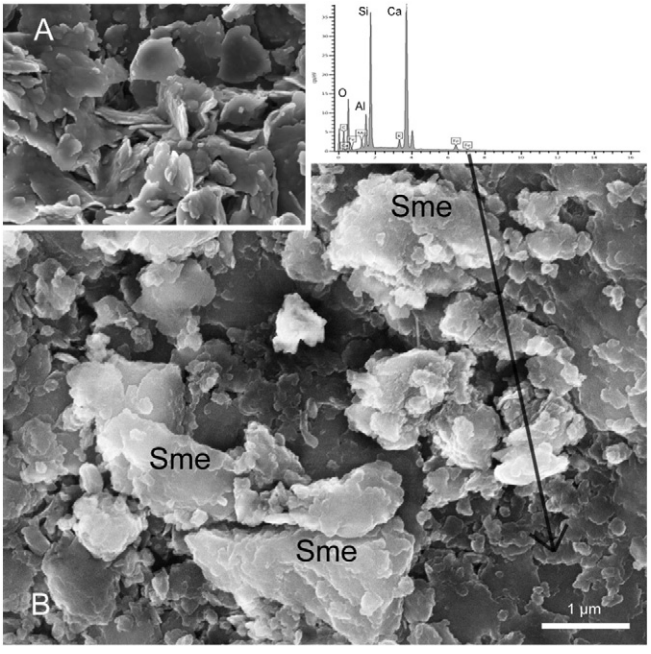

Fig. 5. SEM Secondary electron images and EDX spectrum of A) Untreated sample and B) Sample treated with 15 wt% calcitic lime during 201 days.

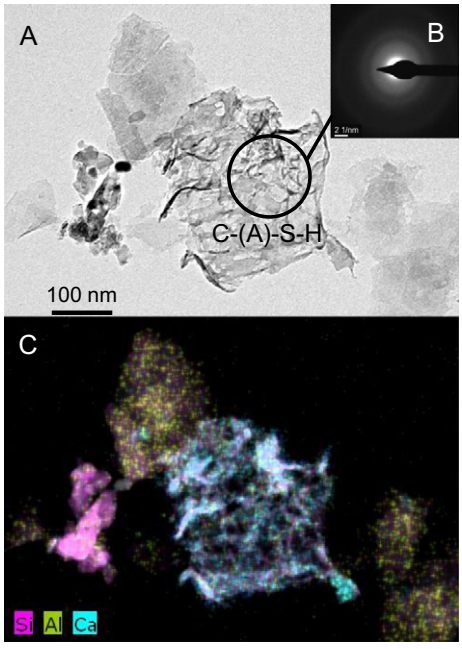

Fig. 6. A) TEM image of C-(A)-S-H in a sample treated with 15 wt% calcitic lime for 7 days. B) Selected area electron diffraction showing the amorphous character of C-(A)-S-H. C) Chemical map corresponding to image A.

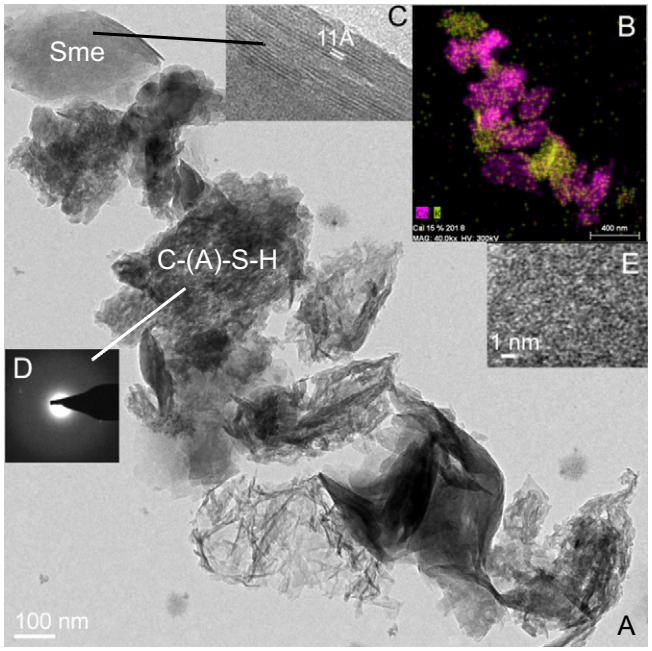

Fig. 7. A) Low magnification TEM image representative of the mixed grains found in the sample treated with 15 wt% calcitic lime during 201 days, composed by smectite crystals encompassed by amorphous C-(A)-S-H. B) Chemical map corresponding to image A. C) High resolution TEM image of smectite (Sme). D) Selected area electron diffraction showing the amorphous character of C-(A)-S-H. E) High resolution TEM image of the C-(A)-S-H.

the treatment (Figs. 6 and 7D–E). Note that the amorphous nature of these phases made their identification by XRD impossible.

4.2. Physical changes upon lime treatment

Surface area and particle size data revealed that flocculation of clay particles occurred immediately upon lime treatment, inducing a drastic surface area decrease and an increase in average particle size. Mowafy et al. (1985) explained that the presence of an electrolyte facilitates the flocculation of colloidal clay particles, resulting in their aggregation and, thus, in a surface area decrease. According to Van Olphen (1987), the range of electrical double layer repulsion between particles decreases with increasing electrolyte concentration. This finding is consistent with the tendency observed here in treated marl samples, showing a more significant decrease in surface area at higher lime concentrations, calcitic lime always being more effective than magnesium-rich lime (Table 4). A lower flocculation efficacy of Mg as compared with Ca has been recognized by Dontsova and Norton (2001), who explained that the higher hydration energy and, thus, the greater hydration radius

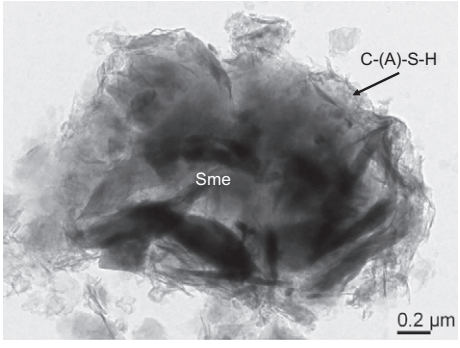

Fig. 8. TEM image of smectite (Sme) surrounded by C-(A)-S-H in a sample treated with 15 wt% Mg-rich lime for 201 days.

Table 7
Chemical composition (AEM-TEM) of C-(A)-S-H phases from marl treated with 15 wt% calcitic lime for 201 days.

Analysis	Si	Al	Fe	Mg	Ca
1	1.00	0.08	0.02	0.00	1.29
2	1.00	0.07	0.04	0.03	0.29
3	1.00	0.09	0.02	0.00	0.61
4	1.00	0.14	0.02	0.00	0.31
5	1.00	0.06	0.03	0.00	0.34
6	1.00	0.05	0.02	0.00	0.34
7	1.00	0.07	0.02	0.00	0.50

of Mg resulted in a larger separation distance and lower attraction between clay particles.

After 1-week of treatment, the surface area of all samples increased by 70–170%. This important increase can be related to the formation of C-(A)-S-H phases which were unambiguously identified with TEM (Figs. 6, 7 and 8). C-S-H phases have an important volume fraction of internal nanopores. These gel pores are responsible for the generally very high surface area of C-S-H phases (Jennings et al., 2008). The increase in particle size after 1 week of treatment provides additional evidence for the presence of C-(A)-S-H, which acted as a cementing material for clay particles, forming larger aggregates. In the sample treated with 5 wt% calcitic lime no C-(A)-S-H phases were detected at any stage of the treatment. Consequently, the particle size did not increase beyond the initial flocculation effect. This is not surprising because the pH was too low to facilitate sufficient mineral dissolution and C-(A)-S-H formation. The result suggest that in this case the observed high surface area is mainly due to dispersed smectite particles, which did not form aggregates as in samples treated with higher lime concentrations. Overall, it can be concluded that the particle size increase was not only induced by flocculation, but, more significantly, by cementation due to C-(A)-S-H phase formation.

4.3. Geotechnical changes upon treatment

The soil's physical properties are largely controlled by the type and amount of clay minerals (Eades and Grim, 1960). Considering a smectite content of ~30% in the marly clay tested here, the values obtained for plastic limit and plasticity index (24.3 and 42.7, respectively) are within the range of typically reported values for montmorillonite (i.e., 40–100 and 100–500, respectively; Bain 1971). According to the Unified Soil Classification System (USCS) the marl can be classified as clay with high plasticity (CH). Experimental results revealed improvements of the marl's geotechnical properties upon lime treatments, indicated by a decrease in plasticity index, free swell, and swelling pressure. These improvements are mainly caused by textural changes during the lime treatment, which are reflected by an increase in particle size. Commonly, cation exchange and flocculation are thought to be primarily responsible for short-term improvements of the subgrades´ geotechnical properties. Pozzolanic reactions resulting in C-(A)-S-H precipitation, in contrast, are described as slow processes which would not significantly contribute to short-term improvement (Little and Nair, 2009). Results reported here indicate that the instant flocculation effect caused only a limited increase in particle size and that the formation of clay/C-S-H aggregates detected after only one week of treatment was more effective in augmenting the particle size. It can be concluded that the formation of pozzolanic phases acting as cementing material was crucial in the improvement of the marl's geotechnical properties observed here, causing a decrease in plasticity index and swelling pressure. Note that the sample treated with 5 wt% calcitic lime, which did not experience C-(A)-S-H formation, showed no decrease in plasticity index. It is also important to keep in mind that flocculation is a reversible process and an at least partial deflocculation might occur if the electrolyte concentration decreases. Karnland et al. (2007) were able to prove that the swelling pressure of Wyoming bentonite increased again when the

electrolyte (i.e. 1 M NaCl) was replaced by water. Aggregation by C-S-H formation, in contrast, can be considered irreversible, unless a decomposition of the cementing C-S-H phases occurs (see below). These results suggest that the formation of pozzolanic phases is essential to assure long-term stabilization of subgrades.

4.4. pH evolution upon lime treatment

pH is an important indicator for the effectiveness of lime treatments. Bell (1996) recognized the pH dependence of aluminosilicate dissolution and pozzolanic reactions and concluded that in the case of soil stabilization using lime, a pH ~12.4 (i.e., pH of saturated $Ca(OH)_2$ solution) should be maintained to achieve maximum reactivity. Several reactions including the aforementioned mineral dissolution, the formation of C-S-H phases, and the carbonation of $Ca(OH)_2$ will consume OH^- groups and result in a pH decrease (Gaucher and Blanc, 2006). The dissolved silicate and aluminate species react with Ca and form C-S-H, C-A-H, and/or C-A-S-H phases (i.e., pozzolanic reaction products). However, below pH 11 clay mineral dissolution is significantly reduced (Huertas et al., 2009, Köhler et al. 2005) and pozzolanic reactions will, thus, be limited.

The experimental results of the pH evolution upon treatments with lime concentrations ≤10 wt% showed a fast decrease during the first 50 days of the test. The comparatively low $Ca(OH)_2$ concentrations used in these tests resulted in a limited amount of available OH^- groups which was partially consumed by the aforementioned mineral reactions. In contrast, the slower pH decrease observed in tests using 15 wt% of lime is due to a larger amount of OH^- groups available for mineral reactions. However, marl treated with 15 wt% magnesium-rich lime experienced a faster pH decrease than marl treated with 15 wt% calcitic lime. This can be explained by the lower amount of available OH^- groups in the former lime, caused by the presence of $Mg(OH)_2$. Note that the solubility of $Mg(OH)_2$ is more than two orders of magnitude lower than the one of $Ca(OH)_2$, resulting in a pH 10.4 for saturated $Mg(OH)_2$ solution.

pH has also a strong influence on the stability of C-S-H phases. During the early stage of the lime treatment, the pH is buffered at ~12.4 by $Ca(OH)_2$ and C-S-H phases are stable. Once the pH decreases due to the aforementioned mineral reactions, C-S-H phases will start to carbonate and decompose into calcite and silica gel (Baston et al., 2012). Carbonation of C-S-H phases depends, however, on their chemical composition. Some pozzolanic phases are reported to remain stable at pH 10.18 (Aguilera et al., 2003). At pH ~9, calcite will be the dominant phase in lime treated soil.

Carbonation of C-S-H is likely to have a negative effect on the geotechnical properties of stabilized soil over time. Research on the degradation mechanisms of Portland cement showed that the carbonation of C-S-H phases led to the formation of a highly permeable silica gel layer, which had poor mechanical integrity (Huet et al., 2010). The second phase formed upon C-S-H carbonation is calcite, the cementing material in lime mortars. The comparison of the compressive strength of common aerial and hydraulic lime mortars (i.e., <2 N/mm^2 for aerial lime mortar and 3–13 N/mm^3 for hydraulic lime mortar, depending on the degree of hydraulicity (Costigan and Pavía, 2012)) evidences the influence of pozzolanic phases on mechanical strength. Increased mechanical strength is an important aspect of lime treatments. This is of paramount importance in the case of soil with high smectite content, which will require strong bonding of clay particles by cementing material to counteract dimensional changes upon expansion and contraction.

4.5. Application of lime treatments for marly clays

The reduction in particle size detected between 3 and 6 months in lime treated marls implies a possible degradation of the stabilization effect and, thus, questions the effectiveness of the treatment. The experimental results also explain findings reported by Ureña et al. (2015), showing an increase in plasticity index and free swell as well as a decrease in mechanical strength of lime-treated marls after 6 months. The disaggregation of clay particles observed here might be caused by the partial dissolution of C-(A)-S-H phases upon pH reduction. The premature degradation of the stabilization effect can be related with the mineralogical composition of marly clays. The high carbonate content in marls can influence the stability of C-(A)-S-H which have formed upon lime stabilization. Hodgkinson and Hughes (1999) reported on the presence of large amounts of C-S-H gel in Roman mortar from Hadrian's Wall, UK. These phases persisted in the more compact, less porous mortar, whereas elsewhere the cement paste underwent complete carbonation. The authors concluded that C-S-H phases would remain uncarbonated if protected from atmospheric CO_2 or carbonate-bearing groundwater. Diffusion of atmospheric CO_2 can be limited significantly if a sufficiently high moisture content is maintained in the marl during lime treatment. Cizer et al. (2010) studied carbonation and pozzolanic reactions in hydraulic lime mortars and observed that carbonation was favored at 60% RH where mortar pores were only partially filled with water and the diffusion and dissolution of atmospheric CO_2 was facilitated. Pozzolanic reactions, in contrast, were promoted at >90% RH where the mortar's high moisture content inhibited CO_2 diffusion significantly. The protection of C-S-H phases from carbonate-bearing groundwater, however, is very difficult to achieve, especially in the case of marly clays. Berner (1992) provided experimental results, which clearly showed that C-S-H degradation was much faster in marl-type groundwater as compared to pure water. In the former type of groundwater, carbonates act as a buffer and impede an increase in pH. In pure water, in contrast, the pH will increase more rapidly and C-S-H dissolution will occur at a lower rate. The faster carbonation of C-S-H phases in lime-stabilized marls can result in the disaggregation of clay particles, as indicated by granulometry data presented here, inducing the deterioration of geotechnical properties (i.e., increase in plasticity index and swelling pressure).

5. Conclusions

Experimental results revealed an initial improvement of the geotechnical properties of marly clays upon lime treatment. This improvement was caused by a flocculation process and aggregation induced by C-S-H formation. Granulometry results showed that the latter process was imperative in increasing the particle size and, thus, improving geotechnical properties (i.e., decrease in plasticity index and free swell). C-(A)-S-H phases formed at an early stage during lime stabilization. TEM images revealed that clay particles were completely surrounded by C-(A)-S-H phases after 7 days of treatment. Further treatment, however, did not contribute to a significant increase in the amount of cementing phases. XRD, SEM, and TEM results suggest that neither the smectite content was drastically reduced, nor its composition changed. Morphological changes were not detected in treated smectite, implying that dissolution and pseudomorphic substitution by C-(A)-S-H was limited to a very thin superficial layer of the clay particle. Prolonged lime treatment caused a particle size decrease in the marly clay, which will, most likely, result in a degradation of geotechnical properties. The premature particle size decrease can be related to the high carbonate content in marls, which promotes C-(A)-S-H dissolution. These findings question the long-term effectiveness of lime stabilization for marly clays using commonly applied treatment protocols. Further studies will have to be conducted to determine whether changes in the treatment procedure (i.e., higher lime concentrations, longer curing times, maintaining higher moisture levels during treatment, or alternative stabilization agents) would provide more reliable, long-term stabilization of marly clays.

Acknowledgement

The authors wish to thank the personnel of the Centro de Instrumentación Científica (University of Granada) for assistance with TEM, FESEM, TG, granulometry, and elemental analyses. We also

thank Dr. Carlos Rodriguez Navarro for the revision of the manuscript. Financial support has been provided by the Spanish Government (Grant CGL 2015-70642-R) and the Junta de Andalucía (Research Group RNM-179).

References

AENOR, 1993. UNE 103104 Determinación del límite plástico de un suelo.

AENOR, 1994. UNE 103103 Determinación del límite líquido de un suelo por el método del aparato de Casagrande.

AENOR, 1996. UNE 103602 Ensayo para calcular la presión de hinchamiento de un suelo en edómetro.

AENOR, 2011. UNE-EN 459-1 Cales para la construcción. Parte 1: Definiciones, especificaciones y criterios de conformidad.

Aguilera, J., Blanco-Varela, M.T., Martinez-Ramirez, S., 2003. Thermodynamic modelling of the CaO-SiO_2-$CaCO_3$-H_2O closed and open system at 25 °C. Mater. Constr. 53, 35–43.

Al-Mukhtar, M., Khattab, S., Alcover, J.-F., 2012. Microstructure and geotechnical properties of lime-treated expansive clayey soil. Eng. Geol. 139-140, 17–27.

ASTM, 2004. ASTM D2435 Standard Test Methods for One-Dimensional Consolidation Properties of Soils Using Incremental Loading.

ASTM, 2012. ASTM D698-12e2 Standard Test Method for Laboratory Compaction Characteristics of Soil Using Standard Effort (12400 ft-lbf/ft^3 (600 kN-/m^3)).

Azañón, J.M., Azor, A., Yesares, J., Tsige, M., Mateos, R.M., Nieto, F., Delgado, J., López-Chicano, M., Martín, W., Rodríguez-Fernández, J., 2010. Regional-scale high-plasticity clay-bearing formation as controlling factor on landslides in Southeast Spain. Geomorphology 120, 26–37.

Bain, J.A., 1971. A plasticity chart as an aid to the identification and assessment of industrial clays. Clay Miner. 9, 1–17.

Basma, A.A., Tuncer, E.R., 1991. Effect of lime on volume change and compressibility of expansive clays. Transp. Res. Rec. 1295, 52–61.

Baston, G.M.N., Clacher, A.P., Heath, T.G., Hunter, F.M.I., Smith, V., Swanton, S.W., 2012. Calcium silicate hydrate (C-S-H) gel dissolution and pH buffering in a cementitious near field. Mineral. Mag. 76, 3045–3053.

Bell, F.G., 1996. Lime stabilization of clay minerals and soils. Eng. Geol. 42, 223–237.

Berner, U.R., 1992. Evolution of pore water chemistry during degradation of cement in a radioactive waste repository environment. Waste Manag. 12, 201–219.

Biagioni, C., Banaccorsi, E., Lezzerini, M., Merlino, S., 2016. Thermal behaviour of Al-rich tobermorite. Eur. J. Mineral. 28, 5–13.

Bourgois, J., Chauve, P., Didon, J., 1974. La formation d'argiles a blocs dans la province de Cadix, Cordilleras Betiques, Espagne. Reun. Annu. Sci. Terre 2, 79.

Brunauer, S., Emmett, P.H., Teller, E., 1938. Adsorption of gases in multimolecular layers. J. Am. Chem. Soc. 60, 309–319.

Carroll, D., Starkey, H.C., 1971. Reactivity of clay minerals with acids and alkalines. Clay Clay Miner. 19, 321–333.

Cizer, Ö., van Balen, K., van Gemert, D., 2010. Competition between hydration and carbonation in hydraulic lime and lime-pozzolana mortars. Adv. Mater. Res. 133-134, 241–246.

Cliff, G., Lorimer, G.W., 1975. The quantitative analysis of thin specimens. J. Microsc. 103, 203–207.

Costigan, A., Pavía, S., 2012. Influence of the mechanical properties of lime mortar on the strength of brick masonry. In: Válek, J., Hughes, J.J., Groot, C.J.W.P. (Eds.), RILEM Bookseries Vol. 7 Historic Mortars. Springer, Netherlands, pp. 359–372.

Dontsova, K., Norton, L.D., 2001. Effects of exchangeable Ca:Mg ratio on soil clay flocculation, infiltration and erosion. In: Stott, D.E., Mohtar, R.H., Steinhard, G.C. (Eds.), Sustaining the Global Farm. Selected papers from the 10th International Soil Conservation Organization Meeting. Purdue University and USDA-ARS National Soil Erosion Research Laboratory, Indiana, USA, pp. 580–585.

Eades, J.L., Grim, R.E., 1960. Reaction of hydrated lime with pure clay minerals in soil stabilization. Highways Research Board Bulletin 262, 51–63.

Gaucher, E.C., Blanc, P., 2006. Cement/clay interactions – a review: experiments, natural analogues, and modeling. Waste Manag. 26, 776–788.

Ghobadi, M.H., Abdilor, Y., Babazadeh, R., 2014. Stabilization of clay soils using lime and effect of pH variations on shear strength parameters (2014). Bull. Eng. Geol. Environ. 73 (2), 611–619.

Guney, Y., Sari, D., Cetin, M., Tuncan, M., 2007. Impact of cyclic wetting-drying on swelling behavior of lime-stabilized soil. Handbook of Environmental Chemistry. Volume 5: Water Pollution 42, pp. 681–688.

Hodgkinson, E.S., Hughes, C.R., 1999. The mineralogy and geochemistry of cement/rock reactions: high-resolution studies of experimental and analogue materials. In: Metcalfe, R., Rochelle, C.A. (Eds.), Chemical Containment of Waste in the Geosphere. Geol. Soc. Lond. Spec. Pub Vol. 157, pp. 195–211.

Huet, B.M., Prevost, J.H., Scherer, G.W., 2010. Quantitative reactive transport modeling of Portland cement in CO_2-saturated water. International Journal of Greenhouse Gas Control 4, 561–574.

Huertas, F.J., Chou, L., Wollast, R., 1999. Mechanism of kaolinite dissolution at room temperature and pressure: Part II Kinetic study. Geochim. Cosmochim. Acta 63, 3261–3275.

Huertas, F.J., Hidalgo, A., Rozalen, M.L., Pellicione, S., Domingo, C., Garcia Gonzalez, C.A., Andrade, C., Alonso, C., 2009. Interaction of bentonite with supercritically carbonate concrete. Appl. Clay Sci. 42, 488–496.

Jennings, H.M., Bullard, J.W., Thomas, J.J., Andrade, J.E., Chen, J.J., Scherer, G.W., 2008. Characterization and modelling of pores and surfaces in cement paste: correlations to processing and properties. J. Adv. Concr. Technol. 6, 5–29.

Karnland, O., Olsson, S., Nilsson, U., Sellin, P., 2007. Experimental determined swelling pressures and geochemical interactions of compacted Wyoming bentonite with highly alkaline solutions. Phys. Chem. Earth 32, 275–286.

Köhler, S.J., Bosbach, D., Oelkers, E.H., 1997-2006. Do clay mineral dissolution rates reach steady state? Geochim. Cosmochim. Acta 69, 2005.

Lamas, F., Irigaray, C., Chacón, J., 2002. Geotechnical characterization of carbonate marls for construction of impermeable dam cores. Eng. Geol. 66, 283–294.

Little, D.N., Nair, S., 2009. Recommended practice for stabilization of subgrade soils and base materials. NCHRP Web-only Document . Transportation Research 144. Board of the National Academies (57pp).

Moore, D.M., Reynolds, R.C., 1989. X-ray diffraction and the identification and analysis of clay minerals. Oxford University Press, Oxford 322p.

Mowafy, Y.M., Bauer, G.E., Sakeb, F.H., 1985. Treatment of expansive soils: a laboratory study. Transp. Res. Rec. 1032, 34–39.

Nalbantoglu, Z., Tuncer, E.R., 2001. Compressibility and hydraulic conductivity of a chemical treated expansive clay. Can. Geotech. J. 38, 154–160.

Nieto, F., Ortega-Huertas, M., Peacor, D., Arostegui, J., 1996. Evolution of illite/smectite from early diagenesis through incipient metamorphism in sediments of the Basque-Cantabrian Basin. Clay Clay Miner. 44, 304–323.

Nieto, F., Abad, I., Azañon, J.M., 2008. Smectite quantification in sediments and soils by thermogravimetric analysis. Appl. Clay Sci. 38, 288–296.

Obuzor, G.N., Kinuthia, J.M., Robinson, R.B., 2012. Soil stabilisation with lime-activated-GGBS—a mitigation to flooding effects on road structural layers/embankments constructed on floodplains. Eng. Geol. 151, 112–139.

Ouhadi, V.R., Yong, R.N., 2003. The role of clay fractions of marly soils on their post stabilization failure. 70, 365–375.

Ouhadi, V.R., Yong, R.N., Amiri, M., Ouhadi, M.H., 2014. Pozzolanic consolidation of stabilized soft clays. Appl. Clay Sci. 95, 111–118.

Petschick, R., 2010. MacDiff 4.2.6. http://www.geologie.uni-rankfurt.de/Staff/Homepages/Petschick/Classicsoftware.html.

Putnis, A., 2009. Mineral replacement reactions. Rev. Mineral. Geochem. 70, 87–124.

Richardson, I.G., 2008. The calcium silicate hydrates. Cem. Concr. Res. 38, 137–158.

Richardson, I.G., 2014. Model structures for C-(A)-S-H(I). Acta Crystallographica Section B B70, 903–923.

Seco, A., Ramirez, F., Miqueleiz, L., Garcia, B., 2011a. Stabilization of expansive soils for use in construction. Appl. Clay Sci. 51, 348–352.

Seco, A., Ramirez, F., Miqueleiz, L., Garcia, B., Prieto, E., 2011b. The use of non-conventional additives in marls stabilization. Appl. Clay Sci. 51, 419–423.

Sol-Sánchez, M., Castro, J., Ureña, C.G., Azañón, J.M., 2016. Stabilisation of clayey and marly soils using industrial wastes: pH and laser granulometry indicators. Eng. Geol. 200, 10–17.

Ureña, C., Azañón, J.M., Corpas, F., Nieto, F., León, C., Pérez, L., 2013. Magnesium hydroxide, seawater and olive mill wastewater to reduce swelling potential and plasticity of bentonite soil. Constr. Build. Mater. 45, 289–297.

Ureña, C., Azañón, J.M., Corpas, F.A., Salazar, L.M., Ramírez, A., Rivas, F., Mochón, I., Sierra, M.J., 2015. Construcción de un terraplén con suelo estabilizado mediante el uso de agentes alternativos en la Autovía del Olivar. Carreteras 203, 63–72.

van Olphen, H., 1987. Dispersion and flocculation. In: Newman, A.C.D. (Ed.), Chemistry of Clay Minerals, Mineralogical Society Monograph No.6. Longman Scientific & Technical, London, pp. 203–224.

Whitney, D.L., Evans, B.W., 2010. Abbreviations for names of rock-forming minerals. Am. Mineral. 95, 185–187.

Zauyah, S., Schaefer, C.E.G.R., Simas, F.N.M., 2010. Saprolites. In: Stoops, G., Marcelino, V., Mees, F. (Eds.), Interpretation of Micromorphological Features of Soils and Regoliths. Elsevier, Amsterdam, pp. 49–68.